BJP British Journal of Pharmacology

DOI:10.1111/bph.13241
www.brjpharmacol.org

RESEARCH PAPER

Dysregulated post-transcriptional control of COX-2 gene expression in gestational diabetic endothelial cells

Luigia Di Francesco[1]*, Melania Dovizio[1]*, Annalisa Trenti[2]*, Emanuela Marcantoni[1]*, Ashleigh Moore[3], Peadar O'Gaora[4], Cathal McCarthy[4], Stefania Tacconelli[1], Annalisa Bruno[1], Sara Alberti[1], Salvatore Gizzo[5], Giovanni Battista Nardelli[5], Genny Orso[6], Orina Belton[4], Lucia Trevisi[2], Dan A Dixon[3] and Paola Patrignani[1]

[1]*Department of Neuroscience Imaging and Clinical Sciences, Center of Excellence on Aging (CeSI), G. d'Annunzio University, Chieti, Italy, Departments of* [2]*Pharmaceutical and Pharmacological Sciences,* [5]*Women's and Children's Health, University of Padua, Padua, Italy,* [3]*Department of Cancer Biology, University of Kansas Cancer Center, Kansas City, KS, USA,* [4]*School of Biomolecular and Biomedical Science, Conway Institute, UCD, Dublin, Ireland, and* [6]*E. MEDEA Scientific Institute, Conegliano, Treviso, Italy*

Correspondence
Professor Paola Patrignani, Department of Neuroscience, Imaging and Clinical Sciences, Center of Excellence on Aging (CeSI), G. d'Annunzio University, Via deiVestini, 31, 66100 Chieti, Italy. E-mail: ppatrignani@unich.it

*These authors contributed equally.

Received
10 February 2015
Revised
2 June 2015
Accepted
25 June 2015

BACKGROUND AND PURPOSE

Hyperglycaemic memory describes the progression of diabetic complications during subsequent periods of improved glycaemia. We addressed the hypothesis that transient hyperglycaemia causes aberrant COX-2 expression in HUVEC in response to IL-1β through the induction of long-lasting epigenetic changes involving microRNA-16 (miR-16), a post-transcriptional modulator of COX-2 expression.

EXPERIMENTAL APPROACH

Studies were performed on HUVEC collected from women with gestational diabetes mellitus (GDM) (dHUVEC) and normal women (nHUVEC).

KEY RESULTS

In dHUVEC treated with IL-1β, the expression of COX-2 mRNA and protein was enhanced and generation of prostanoids increased (the most abundant was the promitogenic $PGF_{2\alpha}$). COX-2 mRNA was more stable in dHUVEC and this was associated with miR-16 down-regulation and c-Myc induction (a suppressor of miR expression). dHUVEC showed increased proliferation in response to IL-1β, which was prevented by a COX-2 inhibitor and $PGF_{2\alpha}$ receptor antagonist. Comparable changes in COX-2 mRNA, miR-16 and c-Myc detected in dHUVEC were produced in nHUVEC exposed to transient high glucose and then stimulated with IL-1β under physiological glucose levels; superoxide anion production was enhanced under these experimental conditions.

CONCLUSIONS AND IMPLICATIONS

Our results describe a possible mechanism operating in GDM that links the enhanced superoxide anion production and epigenetic changes, associated with hyperglycaemic memory, to endothelial dysfunction through dysregulated post-transcriptional control of COX-2 gene expression in response to inflammatory stimuli. The association of conventional

therapy for glycaemic control with agents affecting inflammatory responses and oxidative stress might lead to a more effective prevention of the complications associated with GDM.

Abbreviations

ARE, uridylate-rich region; FP, $PGF_{2\alpha}$ receptor; GDM, gestational diabetes mellitus; miRNA, microRNA; NAC, N-acetylcysteine; PGI_2, prostacyclin; TP, TXA_2 receptor; TX, thromboxane; UTR, 3′ untranslated region

Tables of Links

TARGETS	
GPCRs[a]	**Enzymes**[b]
FP receptor	COX-1
TP receptor	COX-2
	HDAC3

LIGANDS		
AL-8810	PGD_2	PGI_2 (prostacyclin)
D-glucose	PGE_2	SQ29548
IL-1β	$PGF_{2\alpha}$	TNF-α
Leptin	PGH_2	TXA_2

These Tables list key protein targets and ligands in this article which are hyperlinked to corresponding entries in http://www.guidetopharmacology.org, the common portal for data from the IUPHAR/BPS Guide to PHARMACOLOGY (Pawson *et al.*, 2014) and are permanently archived in the Concise Guide to PHARMACOLOGY 2013/14 ([a,b]Alexander *et al.*, 2013a,b).

Introduction

A relationship between maternal gestational diabetes mellitus (GDM) and the risk of metabolic and cardiovascular disease in the offspring has been reported (Yessoufou and Moutairou, 2011; Marco *et al.*, 2012). Intrauterine exposure seems to allow the 'transmission' of diabetes to the offspring (Yessoufou and Moutairou, 2011; Marco *et al.*, 2012). In GDM, the increased glucose levels in the maternal circulation are transported to the fetoplacental circulation (Hay, 2006) and this induces pathophysiological changes, which persist even when maternal hyperglycaemia is corrected due to a phenomenon known as metabolic memory (Zhang and Wu, 2014).

There is accumulating evidence supporting the notion that epigenetic changes, which comprise post-translational histone modifications, DNA methylation and expression of microRNAs (miRNAs), confer the ability of the cell to 'memorize' the alterations in gene activation and cell phenotype induced by exposure to a diabetic milieu *in vivo* (Cooper and El-Osta, 2010; Jayaraman, 2012).

The function of fetoplacental endothelial cells has been found to be abnormal in GDM (Leach, 2011; Sobrevia *et al.*, 2011). These cells were shown to have enhanced relaxation responses to hypoxia and produced increased contractions to re-oxygenation or hydrogen peroxide and these responses occurred through COX-dependent mechanisms (Figueroa *et al.*, 1993).

Both COX-1 and COX-2 are expressed in endothelial cells and catalyse the formation of prostanoids from arachidonic acid by generating the unstable bicyclic endoperoxide intermediate PGH_2 (Di Francesco *et al.*, 2009). Tissue-specific synthases convert PGH_2 to the parent prostanoids, $PGF_{2\alpha}$, PGE_2, PGD_2, PGI_2 (prostacyclin) and thromboxane (TXA_2) (Patrignani and Patrono, 2015). These molecules then interact with cell surface receptors and induce a variety of biological effects (Patrignani and Patrono, 2015). HUVECs generate and release not only the vasodilators PGI_2 and PGE_2 but also large amounts of the vasoconstrictor $PGF_{2\alpha}$ (Di Francesco *et al.*, 2009).

In GDM, placental transcriptome analysis has shown the activation of multiple signal transduction pathways, involving inflammatory mediators, such as TNF-α, IL-1 and leptin, which may contribute to cell hypertrophy and a dysfunctional vasculosyncytial membrane (Radaelli *et al.*, 2003). These results suggest that the fetus of diabetic mothers develops in an inflammatory milieu.

IL-1β induces different functional changes in normal HUVEC by affecting the expression of many genes associated with apoptosis, the cell cycle, the NF-κB cascade, chemotaxis, immune response and cellular permeability (Williams *et al.*, 2008).

IL-1β is a strong inducer of COX-2 primarily through post-transcriptional regulation of gene expression involving RNA-binding proteins interacting with the uridylate-rich regions (AREs) localized in the 3′ untranslated region (UTR) of COX-2 mRNA (Dixon *et al.*, 2006). Among them, HuR protein (Hu antigen R; ELAVL1) promotes mRNA stabilization of COX-2 under pathological conditions when it translocates from the nucleus to the cytoplasm and binds to the ARE elements of COX-2 mRNA (Brennan and Steitz, 2001; Dixon *et al.*, 2006). Recently, microRNA-16 (miR-16) has been demonstrated to regulate COX-2 expression by targeting the 3′ UTR (Moore *et al.*, 2011), which leads to a concurrent reduction in COX-2 mRNA and protein levels, and PGE_2 biosynthesis in IL-1β-stimulated cells (Young *et al.*, 2012). To date, the role played by miR-16 and HuR in the regulation of COX-2 expression in HUVECs treated with inflammatory stimuli, such as IL-1β, has not been investigated

The objectives of the present study were to address whether (i) HUVECs isolated from GDM women (dHUVEC) are associated with altered regulation of COX-2 expression and enhanced biosynthesis of prostanoids, in response to

IL-1β, in comparison with HUVEC derived from normal women (nHUVEC); (ii) the aberrant expression of COX-2 detected in dHUVEC is associated with changes in HuR localization and miR-16 expression; and (iii) these changes influence the proliferative phenotype. We verified whether these altered responses to IL-1β induced by the GDM environment were produced in nHUVEC transiently exposed to high glucose (HG) levels.

Methods

HUVEC isolation, cell culture conditions and biochemical assessments

Umbilical cords were collected after delivery from four full-term normal or four gestational diabetic pregnancies (Obstetrics and Gynaecological Unit, Padua University Hospital, Italy), treated by diet alone. The women were of comparable age, the study was approved by the local ethics committee and the patients gave their informed consent. This study conforms to the principles outlined in the Declaration of Helsinki for the use of human tissue. The HAPO/IADPSG (Hyperglycemia and Adverse Pregnancy Outcome/International Association of Diabetes and Pregnancy Study Groups) guidelines were used for GDM diagnostic criteria (International Association of Diabetes and Pregnancy Study Groups Consensus Panel, 2010). Patients with basal glycaemia >92 and >180 or >153 mg·dL^{-1} at 1 and 2 h, respectively, after an oral glucose load were diagnosed as having GDM. The GDM group did not show insulin resistance before or after pregnancy.

HUVECs were isolated and grown as previously described (Jaffe *et al.*, 1973; Trevisi *et al.*, 2006; Di Francesco *et al.*, 2009) and used at passage level 2. nHUVEC and dHUVEC were plated in 6-well dishes and allowed to reach confluence (5×10^5 cells). Cells were incubated in the absence or presence of IL-1β (Sigma-Aldrich, Milan, Italy) 5 ng·mL^{-1} dissolved in PBS for 6 and 24 h. The concentration of the cytokine used in the present study is of pathophysiological relevance; in fact, enhanced blood levels of IL-1β have been detected in GDM compared with normal women and they reached a concentration of 2.5 ng·mL^{-1} (Vitoratos *et al.*, 2008). At different time points, we assessed the levels of different proteins, that is, COX-2, COX-1 by specific Western blot techniques (Di Francesco *et al.*, 2009), COX-2 and c-Myc mRNAs and miR-16 by quantitative PCR (qPCR), as previously described (Young *et al.*, 2012; Dovizio *et al.*, 2013). The levels of 6-keto-$PGF_{1\alpha}$ (the hydrolysis product of PGI_2), PGE_2 and $PGF_{2\alpha}$ were measured in cell culture media by previously described and validated radioimmunoassay techniques (Ciabattoni *et al.*, 1979; Patrono *et al.*, 1982; Patrignani *et al.*, 1984; 1994). [^{3}H]-6-keto-$PGF_{1\alpha}$, [^{3}H]-PGE_2 and [^{3}H]-$PGF_{2\alpha}$ (200–250 Ci·mmol^{-1}) were from PerkinElmer (Akron, OH, USA). 6-Keto-$PGF_{1\alpha}$, PGE_2 and $PGF_{2\alpha}$ were purchased from Cayman Chemical (Ann Arbor, MI, USA). Anti-6-keto-$PGF_{1\alpha}$, anti-PGE_2 and anti- $PGF_{2\alpha}$ were obtained in our laboratory and their characteristics were as described previously (Ciabattoni *et al.*, 1979; Patrono *et al.*, 1982; Patrignani *et al.*, 1984). PGD_2 and TXB_2 levels were measured by enzyme immunoassay (Cayman Chemical) according to the protocol of the manufacturer (Di Francesco *et al.*, 2009; Patrignani and Patrono, 2015). For mRNA stability analysis, HUVECs were treated with IL-1β (5 ng·mL^{-1}) for 6 h and then treated with the transcriptional inhibitor actinomycin D (Sigma-Aldrich), dissolved in DMSO to a final concentration of 0.65 μg·mL^{-1}, at the time points indicated.

In some experiments, nHUVECs were transiently exposed to HG (D-glucose, 30 mM) or D-mannitol (30 mM), as an osmotic control, for 16 h, then cells were maintained in normal glucose condition (D-glucose 5.5 mM) for 1 day and subsequently stimulated with IL-1β (5 ng·mL^{-1}) or vehicle for 6 h. In this experimental condition, we assessed the levels of COX-2 and c-Myc mRNAs and miR-16 by qPCR.

Measurement of superoxide levels

The superoxide levels were measured by a commercial kit according to the manufacturer's instructions (Total Superoxide Detection Kit; Enzo Life Sciences, Rome, Italy). nHUVECs (1.5×10^5 cells) were seeded on glass coverslip and transiently exposed to HG (30 mM) or D-mannitol (30 mM) as described earlier. Then cells were incubated with 2 μM of superoxide detection reagent for 30 min at 37°C in the presence or absence of IL-1β (5 ng·mL^{-1}). In some experiments, nHUVECs were pretreated with the antioxidant N-acetylcysteine (NAC) (Enzo Life Sciences) (5 mM) or vehicle for 30 min before the stimulation with IL-1β. Changes in fluorescence intensity were measured using a confocal microscopy (Zeiss LSM 510 Meta, Zeiss International, Oberkochen, Germany) at excitation/emission wavelengths 550/610 nm. The quantification of fluorescence intensity was calculated using the ImageJ1.44 software (NIH, Bethesda, MD, USA).

HUVEC proliferation assays

The effect of IL-1β on the proliferation of nHUVEC and dHUVEC was evaluated using the [^{3}H]-thymidine incorporation assay as previously described (Sexl *et al.*, 1995; Trevisi *et al.*, 2010). HUVECs were plated onto 96-well plates at a density of 5×10^3 cells per well in complete cell culture medium [DMEM-medium199 (50% v.v^{-1}) supplemented with 5% FCS without or with IL-1β for 24 h. In some experiments, the effect of the COX-2 inhibitor NS-398 (1 μM) was evaluated. NS-398 1 μM was previously shown to cause a selective inhibition of COX-2. In fact, it completely suppressed the activity of monocyte COX-2 without affecting platelet COX-1 (Panara *et al.*, 1995). Moreover, we have previously found that this concentration is able to completely suppress COX-2 activity induced in HUVEC by IL-1β (Di Francesco *et al.*, 2009).

In order to verify the involvement of $PGF_{2\alpha}$ and/or TXA_2 in the enhanced cellular proliferation observed in IL-1β-stimulated dHUVEC compared to nHUVEC, we used the MTT [3-(4,5-dimethylthiazol-2-yl)-2,5-diphenyltetrazolium bromide] assay from Cayman Chemical (Mosmann, 1983; Trevisi *et al.*, 2006; Trevisi *et al.*, 2010), which is a widely accepted alternative to the use of the radiochemical assay. nHUVEC and dHUVEC were plated onto 96-well plates at a density of 5×10^3 cells per well in complete cell culture medium [DMEM-medium199 (50% v·v^{-1}) supplemented with 5% FCS] and incubated without or with IL-1β (5 ng·mL^{-1}) for 24 h. dHUVECs were incubated with IL-1β or in the presence of AL-8810 (1 μM), a selective antagonist of the $PGF_{2\alpha}$ recep-

tor (FP) (Griffin *et al.*, 1999). In some experiments, exogenous $PGF_{2\alpha}$ (1 μM) was added. Moreover, we evaluated the effect of the selective TXA_2 receptor (TP) antagonist, SQ29548 (1 and 10 μM) (Ogletree *et al.*, 1985). Four hours before the end of incubation, 10 μL of MTT substrate was added to each well. At the end of the treatment the incubation medium was removed and the formazan crystals were dissolved in 100 μL of crystal-dissolving solution. MTT reduction was quantified by measuring the light absorbance with a multilabel plate counter (Spectra MAX 190, Molecular Devices, Sunnyvale, CA, USA) at 570 nm. Background absorbance from control wells (media without cells) was subtracted.

Confocal microscopy

Cells (8×10^4 per well in 12-well plates containing glass coverslips) were treated with IL-1β (5 ng·mL^{-1}) for 24 h (PBS for control cells). Cells were stained and confocal images were acquired as previously described (Trenti *et al.*, 2014). The antibody mouse anti-HuR (1:100, Santa Cruz Biotechnology, Santa Cruz, CA, USA) was used. The secondary antibody used for immunofluorescence (Alexa Fluor 488 conjugates from Invitrogen) was at 1:500. Nuclear staining was performed with propidium iodide (0.5 μg·mL^{-1}).

miRNA transfection

HUVECs (2×10^5 cells) were seeded in six multi-well plate in complete medium and when they had reached 80% cellular confluence miRNA transfection was accomplished using Lipofectamine 2000 (Applied Biosystems, Foster City, CA, USA), according to the manufacturer's protocol and as previously described (Sun *et al.*, 2012). miR negative control (50 nmol·L^{-1}) (Sigma-Aldrich) or hsa-miR-16 (50 nmol·L^{-1}) (Sigma-Aldrich) was transfected for 24 h before the stimulation with IL-1β (5 ng·mL^{-1}) (Sigma-Aldrich) for 6 h.

RNA analysis

Total RNA was extracted from HUVEC using Trizol reagent (Invitrogen, Carlsbad, CA, USA) according to the manufacturer's protocols. For mRNA levels of COX-2 and c-Myc, 1 μg of total RNA was treated with DNAse kit (Fermentas, St Leon-Rot, Germany) and subsequently reverse transcribed into cDNA using Iscript cDNA synthesis kit (Bio-Rad Laboratories, Hercules, CA, USA) according to the manufacturer's protocols. One hundred nanograms of cDNA was used for the reaction mixture and the amplification of COX-2, c-Myc and GAPDH was performed using iTaqTM Fast SYBR® Green Supermix With ROX (Bio-Rad), and these couples of primers: COX-2 fwd: 5'GCTCAGCCATACAGCAAATCC; rev: 5'CCAAAATC CCCTTGAAGTGGG; c-Myc fwd: 5'TCCTCGGATTCTCTG CTCTC; rev: 5'CTCTGACCTTTTGCCAGGAG; GAPDH fwd: 5'TCACCAGGGCTGCTTTTAAC; rev: 5'GACAAGCTTC-CCGTTCTCAG using 7900HT Fast Real-Time PCR System (Applied Biosystems, Milan, Italy). Gene expression assays were performed by relative quantification with comparative cycle threshold using ABI Prism, SDS 2.1 software (Applied Biosystems). For miR-16 detection, 10 ng of total RNA was converted to cDNA using the TaqMan miRNA reverse transcription kit (Applied Biosystems) with miRNA primers specific for mature hsa-miR-16 and the small nuclear protein RNU6B (U6) control for normalization (Applied Biosystems); qPCR detection of miRNAs was carried out using TaqMan probes designed for miR-16 and U6 (Applied Biosystems).

Statistical analysis

All values are reported as mean ± SEM. Different molecular markers were assessed in separate experiments whose number was chosen according to their coefficient of variation (CV) previously assessed in experiments performed in nHUVEC. Most biomarkers showed a CV of 15–30%. Thus, three to five experiments would allow us to detect a significant difference of 35–100% between two means using *t*-test at significance level (α) of 0.05 (two tailed) with a power of 90%. In contrast, HUVEC prostanoid biosynthesis is characterized by higher CV% (average CV is 60%) (Di Francesco *et al.*, 2009); thus, five to eight experiments would allow us to detect a significant difference of 200–100% between means. Statistical analysis was performed using GraphPad Prism and StatMate Software (version 5.00 for Windows; GraphPad, San Diego, CA, USA). Student's *t*-test was used to compare the means of two independent groups to each other, whereas ANOVA followed by Newman–Keuls post test was used to compare the means of more than two independent groups. Values of $P < 0.05$ were considered statistically significant.

Results

COX-2 protein levels in dHUVEC and nHUVEC

Under unstimulated growth conditions, COX-2 protein levels were low both in dHUVEC and nHUVEC (Figure 1A). Treatment with IL-1β induced COX-2 both in dHUVEC and nHUVEC, with the protein levels consistently higher in dHUVEC as compared with nHUVEC (Figure 1A).

COX-1 levels were comparable in nHUVEC and dHUVEC under basal conditions and were not affected by IL-1β (Supporting Information Fig. S1).

Enhanced biosynthesis of prostanoids in dHUVEC versus nHUVEC

We measured the levels of 6-keto-$PGF_{1\alpha}$ (the hydrolysis product of PGI_2), PGE_2, PGD_2, TXB_2 (the hydrolysis product of TXA_2) and $PGF_{2\alpha}$ in unstimulated HUVEC or in response to IL-1β. The incubation of dHUVEC and nHUVEC with IL-1β was associated with a pronounced increase in the five prostanoids, which were released in a time-dependent fashion (Figure 1B–F). In dHUVEC treated with IL-1β for 6 and 24 h, 6-keto-$PGF_{1\alpha}$ and TXB_2 levels were significantly higher than those detected in the medium of nHUVEC (Figure 1B and E). Similar results were obtained for PGE_2, PGD_2 and $PGF_{2\alpha}$, but the increase was statistically significant only after 24 h of incubation with IL-1β (Figure 1C, D and F). In dHUVEC and nHUVEC, $PGF_{2\alpha}$ was the major prostanoid generated both at baseline and after treatment with IL-1β.

COX-2 mRNA expression in dHUVEC and nHUVEC

As shown in Figure 2A, mRNA levels of COX-2 in dHUVEC were significantly ($P < 0.01$) higher compared with nHUVEC

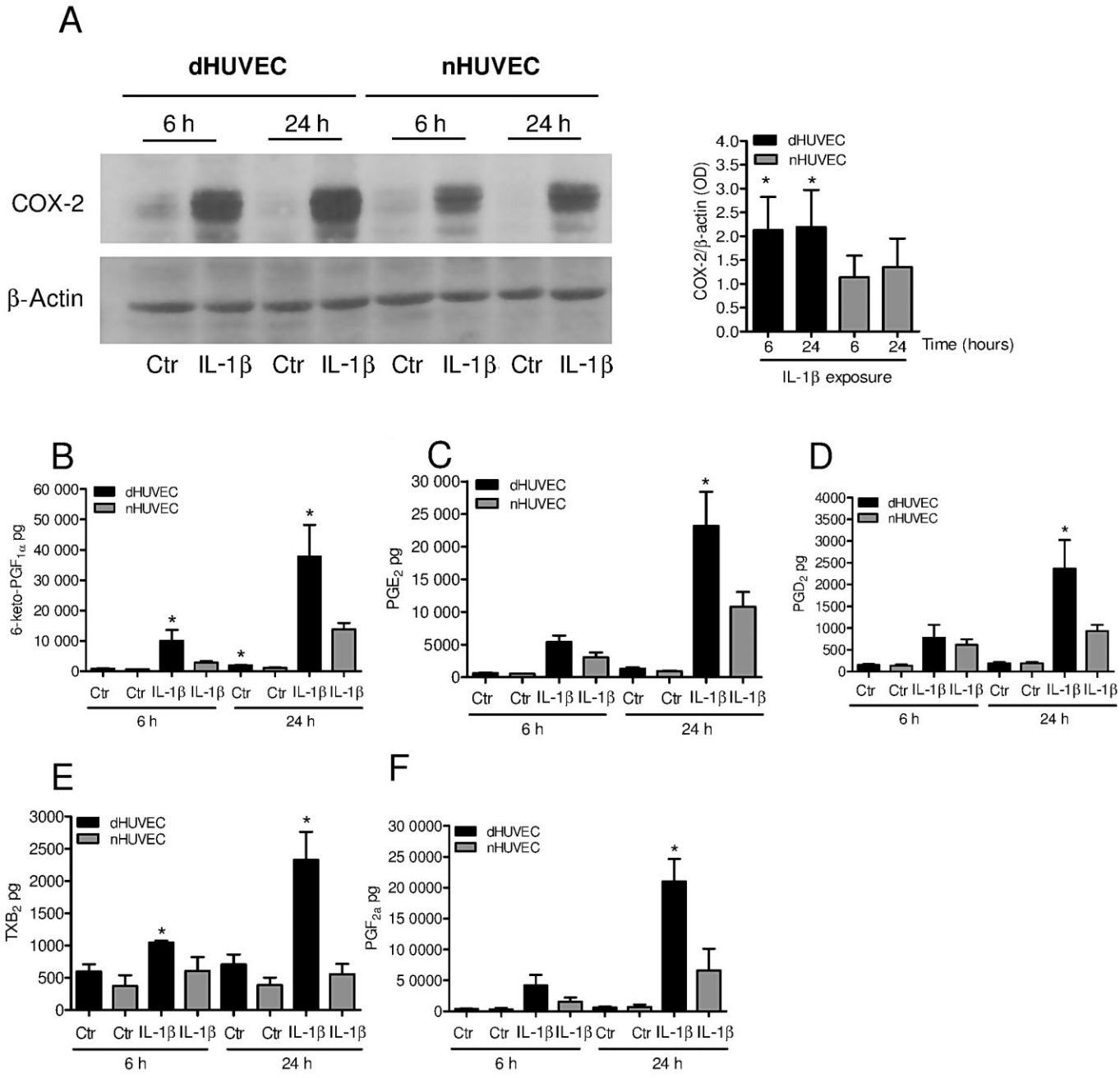

Figure 1

COX-2 protein expression and prostanoid biosynthesis in dHUVEC and nHUVEC in response to IL-1β. (A) COX-2 levels in HUVEC under basal conditions (Ctr) and after stimulation with IL-1β (5 ng·mL^{-1}) for 6 and 24 h, assessed by Western blot. Densitometric analysis of the expression levels of COX-2 (OD value/β-actin OD) detected in the presence of IL-1β, represent mean ± SEM (n = 4–5); *P < 0.05 versus nHUVEC. (B–F) Total amounts of prostanoids produced by dHUVEC and nHUVEC (5×10^5 cells) cultured in the absence or in the presence of IL-1β. Values are presented as mean ± SEM from five to eight separate experiments. *P < 0.05 versus nHUVEC at the same time points.

in response to IL-1β both at 6 and 24 h. In order to verify whether the higher levels of COX-2 transcript detected in dHUVEC stimulated with IL-1β were due to altered mRNA stability, we compared COX-2 mRNA levels in dHUVEC and nHUVEC exposed to IL-1β for 6 h and then treated with actinomycin D to halt transcription and determine mRNA half-life. Figure 2B shows that the COX-2 mRNA was more stable in dHUVEC compared with nHUVEC ($t_{1/2}$ = 92 ± 12.2

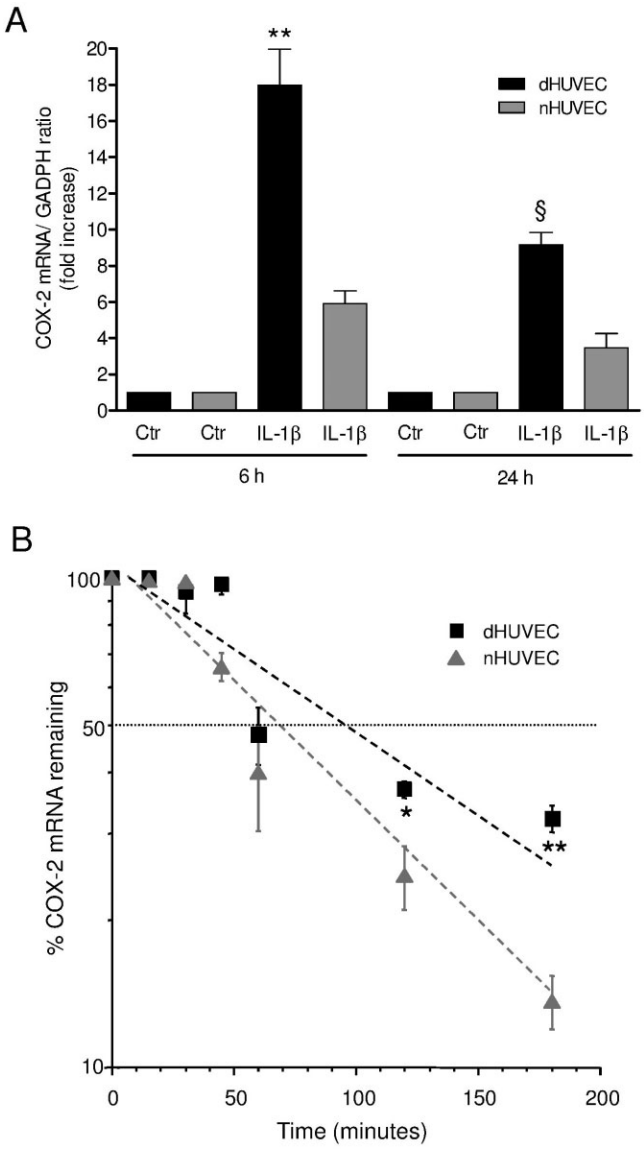

Figure 2

Analysis of COX-2 mRNA levels in nHUVEC and dHUVEC cultured without or with IL-1β. (A) Cells were cultured in basal conditions or treated with IL-1β (5 ng·mL^{-1}) for 6 and 24 h, and COX-2 mRNA expression (normalized to GAPDH) was assessed by qPCR. Values represent fold increase versus control (Ctr); mean ± SEM from three separate experiments; $^{**}P < 0.01$ versus IL-1β, 6 h (nHUVEC) and $^{§}P < 0.01$ versus IL-1β, 24 h (nHUVEC). (B) Assay of COX-2 mRNA stability. Actinomycin D (0.65 μg·mL^{-1}) was added to nHUVEC and dHUVEC cultured for 6 h with IL-1β (5 ng·mL^{-1}), and COX-2 mRNA levels were assessed by qPCR at the indicated time points. Data are presented as mean ± SEM from three separate experiments. $^{*}P < 0.05$ and $^{**}P < 0.01$ versus nHUVEC at the same time points.

vs. 72 ± 10.7 min; $P < 0.05$). Significant differences in COX-2 mRNA levels were observed at 2 and 3 h, with dHUVEC having enhanced COX-2 mRNA levels.

HuR localization in nHUVEC and dHUVEC

Based on its ability to promote COX-2 mRNA stabilization when localized to the cytoplasm, we examined HuR localization in nHUVEC and dHUVEC cultured for 24 h in the absence (baseline condition) and in the presence of IL-1β using confocal microscopy (Figure 3A and B and Supporting Information Fig. S2). In unstimulated conditions, HuR was predominantly localized to the nucleus in both cell types and dHUVEC displayed slightly higher levels of cytoplasmic HuR, as compared with nHUVEC grown under basal conditions (Figure 3A and Supporting Information Fig. S2). In both nHUVEC and dHUVEC, treatment with IL-1β caused an increase in fluorescence intensity of HuR in the cytosolic compartment associated with a decrease in the nuclear HuR signal (Figure 3A and B).

Effect of IL-1β on miR-16 expression in dHUVEC and nHUVEC

In nHUVEC, IL-1β treatment promoted the expression of miR-16 (Figure 3C). In contrast, IL-1β failed to induce miR-16 levels in dHUVEC (Figure 3C). These results indicate that the exposure of HUVEC to a diabetic environment affected the ability of IL-1β to induce miR-16 expression. This phenomenon might contribute to the increase in COX-2 mRNA stability detected in dHUVEC.

To confirm that miR-16 modulates COX-2 expression in endothelial cells, we assessed the effect of transfected mature hsa-miR-16, or a random sequence negative control miRNA, on COX-2 mRNA levels in nHUVEC and dHUVEC exposed to IL-1β. As shown in Figure 3D, overexpression of miR-16 in IL-1β-treated cells suppressed COX-2 mRNA expression both in dHUVEC and nHUVEC.

We assessed c-Myc mRNA levels, a known suppressor of miR-16 (Chang *et al.*, 2008), in dHUVEC and nHUVEC exposed to IL-1β for 24 h. As shown in Figure 3E, IL-1β induced a significant increase in c-Myc in dHUVEC. In nHUVEC, IL-1β slightly decreased the level of c-Myc.

Effect of IL-1β on the proliferation of nHUVEC and dHUVEC

As shown in Figure 4A, IL-1β caused a significant reduction in [^{3}H]-thymidine incorporation both in nHUVEC and dHUVEC. However, the cellular proliferation was significantly higher in dHUVEC compared to nHUVEC (Figure 4A). This difference was prevented by the addition of NS-398 (Figure 4B), suggesting that pro-mitogenic COX-2-dependent prostanoids, such as TXA_2 and/or $PGF_{2\alpha}$, are involved in restraining IL-1β-dependent inhibition of proliferation in dHUVEC.

In order to verify the involvement of the two prostanoids in the enhanced cellular proliferation in response to IL-1β detected in dHUVEC versus nHUVEC, we used selective antagonists of FP and TP receptors, AL-8810 and SQ29548 respectively. We used MTT chromatometry, which is considered to be a convenient, non-radioactive alternative for determining cellular proliferation (Mosmann, 1983). As shown in Figure 4C, AL-8810 (at 1 μM) almost completely abolished the increased cellular proliferation detected in IL-1β-treated dHUVEC compared to nHUVEC. This effect was prevented by the addition of exogenous $PGF_{2\alpha}$ 1 μM (Figure 4C); this concentration is 1.7-fold higher than that endogenously produced after 24 h of incubation with IL-1β (Figure 1F). In contrast, the selective TP antagonist did not affect the

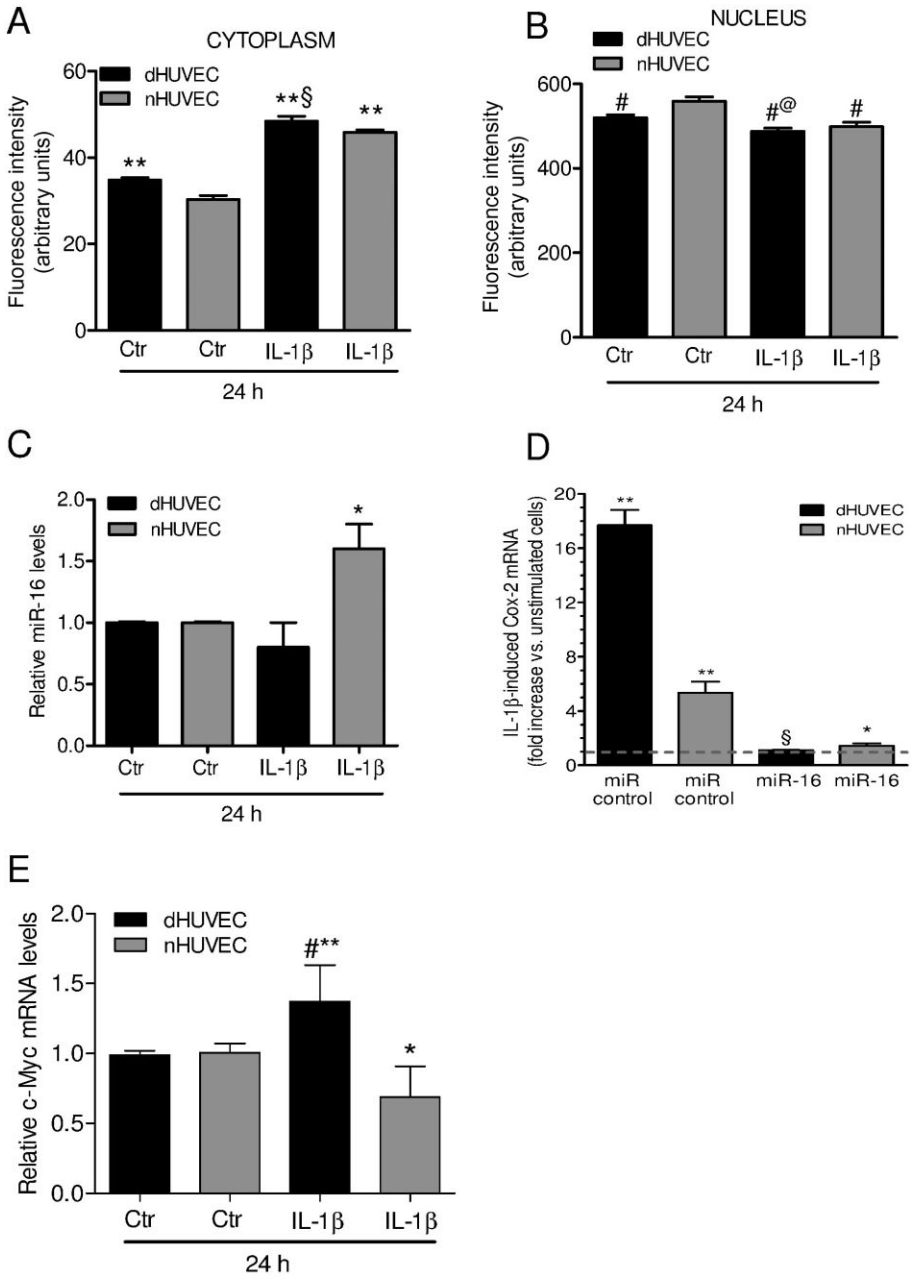

Figure 3

Cellular localization of HuR and the expression of miR-16 and c-Myc in dHUVEC and nHUVEC. (A, B) Cytoplasmic and nuclear localization of HuR by confocal microscopy analysis in nHUVEC and dHUVEC cultured for 24 h in baseline conditions or with IL-1β (5 ng·mL^{-1}). The fluorescence intensity of HuR staining was assessed using Volocity software (version 5.3.2 Improvision Ltd; PerkinElmer). Three separate experiments were performed and for each sample, 10 random fields were collected and analysed. Data are presented as mean ± SEM of three independent experiments; $^{**}P < 0.01$ versus control (Ctr) nHUVEC (untreated with IL-1β), $^{\S}P < 0.01$ versus Ctr dHUVEC, $^{\#}P < 0.01$ versus Ctr nHUVEC, $^{@}P < 0.01$ versus Ctr dHUVEC. (C) Endogenous miR-16 expression in nHUVEC and dHUVEC in response to IL-1β. nHUVEC and dHUVEC were cultured in the absence and presence of IL-1β (5 ng·mL^{-1}) for 24 h, and the levels of miR-16 were assessed by qPCR. Values represent fold increase versus control (Ctr) (i.e. cells cultured in the absence of IL-1β); mean ± SEM from three to four separate experiments, $^{*}P < 0.05$ versus Ctr and IL-1β dHUVEC. (D) miR-16 was transfected into IL-1β-stimulated nHUVEC and dHUVEC and COX-2 mRNA expression was assayed by qPCR and normalized with 18S mRNA levels. Cells were transfected with mature miR-16 or control miR for 24 h and then were stimulated with IL-1β for a further 6 h. Values are presented as mean ± SEM from three to five separate experiments, $^{**}P < 0.01$ nHUVEC and dHUVEC stimulated with IL-1β versus the same cells untreated with IL-1β (unstimulated), $^{*}P < 0.05$ and $^{\S}P < 0.01$ (respectively) versus its own miR control. (E) c-Myc mRNA levels in nHUVEC and dHUVEC in response to IL-1β. nHUVEC and dHUVEC were cultured in the absence and presence of IL-1β (5 ng·mL^{-1}) for 24 h, and the levels of c-Myc mRNA were assessed by qPCR and normalized with GADPH mRNA levels. Values represent fold increase versus control (Ctr) (i.e. cells cultured in the absence of IL-1β); mean ± SEM from three to four separate experiments; $^{*}P < 0.05$ versus Ctr nHUVEC, $^{\#}P < 0.05$ versus Ctr dHUVEC, $^{**}P < 0.01$ versus IL-1β nHUVEC.

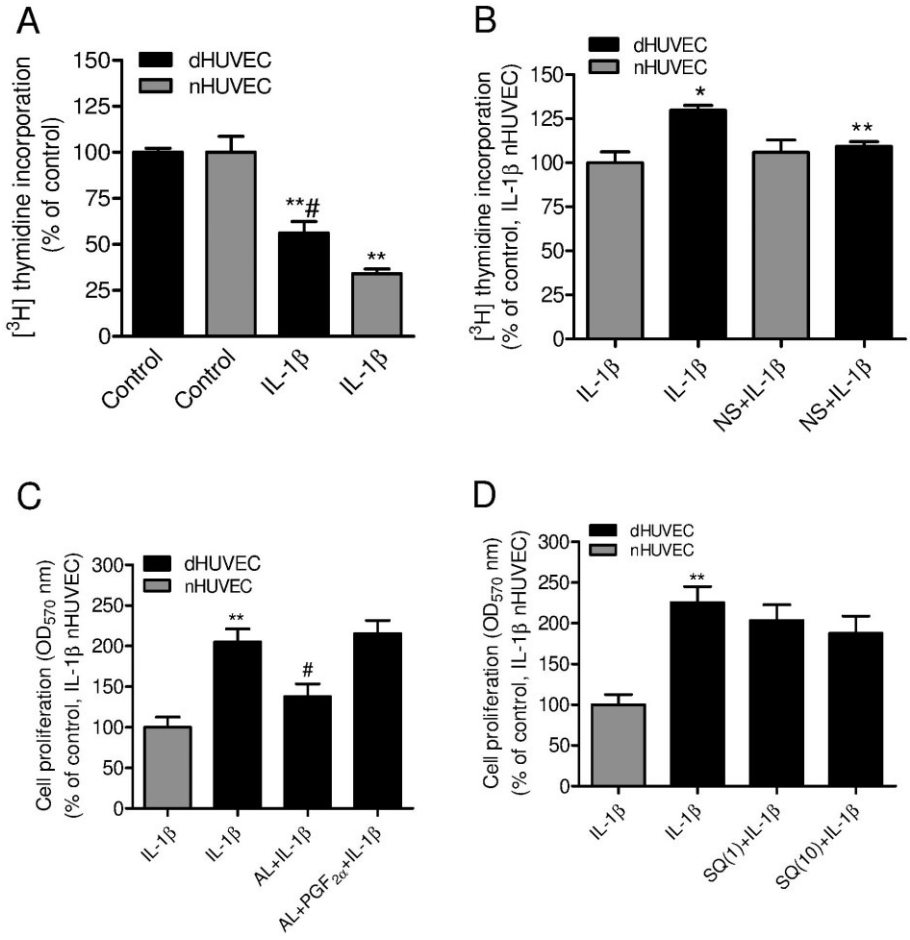

Figure 4

Proliferation of nHUVEC and dHUVEC in response to IL-1β. (A) [^{3}H]-thymidine incorporation into DNA was assayed in nHUVECs and dHUVEC in the absence and in the presence of IL-1β (5 ng·mL^{-1}). Values are presented as % of control (HUVEC cultured under baseline conditions); mean ± SEM, $n = 4$. Each experiment was conducted in quadruplicate, $^{**}P < 0.01$ versus their own controls, $^{\#}P < 0.05$ versus IL-1β nHUVEC. (B) Effect of NS-398 (1 μM) on the proliferation of nHUVEC and dHUVEC cultured in the presence of IL-1β. Values are presented as % of control (i.e. [^{3}H]-thymidine detected in nHUVEC treated with IL-1β and DMSO vehicle); mean ± SEM, $n = 4$. Each experiment was conducted in quadruplicate, $^{*}P < 0.05$ versus nHUVEC-IL-1β, $^{**}P < 0.01$ versus dHUVEC-IL-1β. (C) Effect of the FP antagonist AL-8810 (AL, 1 μM) on the proliferation (by MTT assay, absorbance was measured at 570 nm) of dHUVEC cultured in the presence of IL-1β; in some experiments $PGF_{2\alpha}$ (1 μM) was added. Values are presented as % of control (i.e. absorbance values detected in nHUVEC treated with IL-1β and DMSO vehicle); mean ± SEM, $n = 4$. Each experiment was conducted in quadruplicate, $^{**}P < 0.01$ versus nHUVEC-IL-1β, $^{\#}P < 0.01$ versus dHUVEC-IL-1β and dHUVEC-IL1β + AL + $PGF_{2\alpha}$. (D) Effect of the TP antagonist SQ29548 (SQ, 1 and 10 μM) on the proliferation (MTT assay) of dHUVEC cultured in the presence of IL-1β. Values are presented as % of control (i.e. absorbance values measured by MTT assay in nHUVEC treated with IL-1β and DMSO vehicle); mean ± SEM, $n = 4$. Each experiment was conducted in quadruplicate, $^{**}P < 0.01$ versus nHUVEC-IL-1β.

increased cellular proliferation detected in IL-1β-treated dHUVEC as compared with nHUVEC (Figure 4D).

Altogether these results suggest that an increase in COX-2-dependent $PGF_{2\alpha}$ is involved in the enhanced cell proliferation detected in IL-1β-stimulated dHUVEC versus nHUVEC.

Effect of transient hyperglycaemia on IL-1β-dependent expression of COX-2 mRNA, miR-16 and c-Myc in nHUVEC

To create a model of transient hyperglycaemia, nHUVECs were incubated in high D-glucose (HG) or D-mannitol (30 mM), as an osmotic control, for 16 h and then in physiological glucose levels (5.5 mM) for 1 day; nHUVECs were then stimulated with IL-1β or vehicle for 6 h. Under these experimental conditions, the IL-1β-stimulated increase in COX-2 mRNA levels was significantly higher in nHUVEC exposed to transient HG compared to those treated with D-mannitol (Figure 5A). In nHUVEC transiently exposed to mannitol, IL-1β significantly increased miR-16, but not c-Myc mRNA (Figure 5 B and C respectively). In nHUVEC exposed to HG, IL-1β failed to increase miR-16 (Figure 5B) and this effect was associated with increased levels of c-Myc mRNA (Figure 5C).

Together, these data indicate that transient hyperglycaemia induces long-lasting epigenetic changes in nHUVEC that

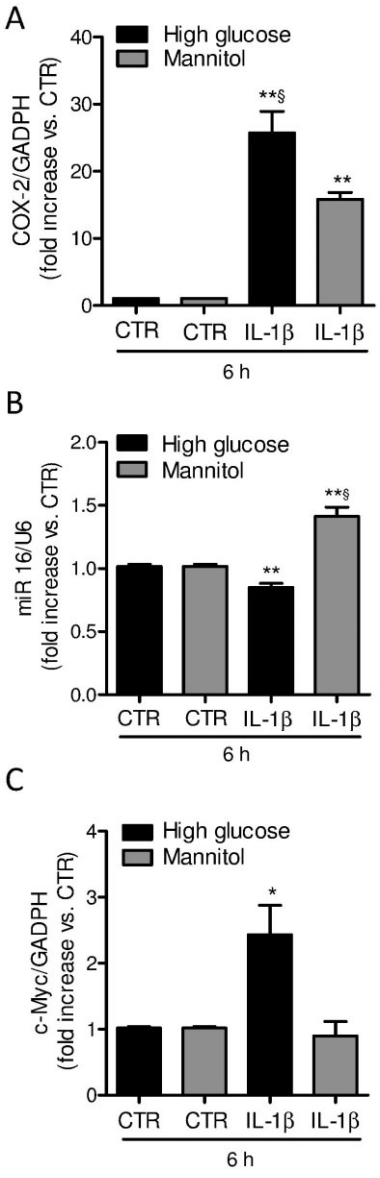

Figure 5

Expression of COX-2, miR-16 and c-Myc in nHUVEC exposed to transient high glucose. In nHUVEC transiently exposed to mannitol (30 mM) or high glucose (30 mM), treated or not with IL-1β (5 ng·mL^{-1}) for 6 h, COX-2 mRNA levels (A), endogenous miR-16 expression (B) and c-Myc mRNA levels (C) were assessed. Data are presented as mean ± SEM of three independent experiments. (A) $^{**}P < 0.01$ versus their own controls (Ctr); $^{§}P < 0.05$ versus IL-1β (mannitol). (B) $^{**}P < 0.01$ versus their own Ctr; $^{§}P < 0.01$ versus IL-1β (high glucose). (C) $^{*}P < 0.05$ versus Ctr and IL-1β (mannitol).

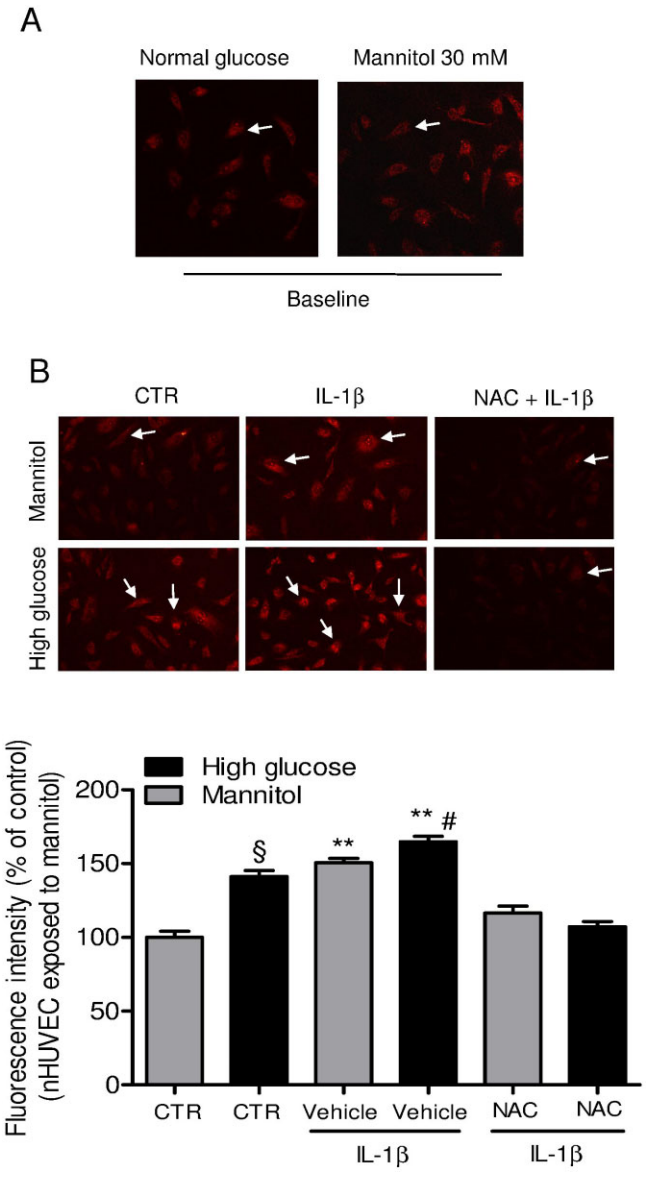

Figure 6

Superoxide generation in nHUVEC exposed to transient high glucose in response to IL-1β. (A) nHUVECs transiently exposed to mannitol (30 mM) or normal glucose (5 mM) were incubated with 2 μM of superoxide detection reagent for 30 min at 37°C. Superoxide generation was detected by confocal microscopy analysis and representative images are shown. Arrows indicate representative positive cells. (B) nHUVECs transiently exposed to mannitol (30 mM) or high glucose (30 mM) were incubated with 2 μM of superoxide detection reagent for 30 min at 37°C in the presence or absence of IL-1β (5 ng·mL^{-1}). NAC (5 mM) was pre-incubated with cells for 30 min before the addition of superoxide detection reagent and IL-1β. The generation of superoxide was assessed by confocal microscopy and quantification of fluorescence intensity was performed using ImageJ software (ver. 1.44). Data are expressed as mean ± SEM from three separate experiments: $^{**}P < 0.01$ versus Ctr and IL-1β + NAC, $^{\#}P < 0.01$ versus IL-1β (mannitol), $^{§}P < 0.01$ versus Ctr (mannitol).

lead to altered COX-2 expression via dysregulation of post-transcriptional mechanisms.

Effect of transient HG on IL-1β-dependent induction of superoxide anion in nHUVEC

Superoxide anion production was assessed in nHUVEC by confocal microscopy using a specific detection kit. As shown in Figure 6A, nHUVEC cultured in physiological glucose

levels (5.5 mM) or in high D-mannitol (30 mM) for 16 h showed a low fluorescence signal. Cells transiently exposed to HG and then cultured in physiological glucose levels were characterized by enhanced superoxide anion production versus nHUVEC transiently exposed to D-mannitol (Figure 6B). After a short incubation (30 min) of nHUVEC with IL-1β, the fluorescence signal was enhanced in nHUVEC pre-exposed to HG or mannitol. However, superoxide anion production was higher in the cells transiently exposed to HG versus those incubated with mannitol (Figure 6B). The fluorescence signal was almost completely abolished by incubation with the antioxidant NAC (Figure 6B) that is known to inhibit NADPH oxidase-mediated increase in superoxide production (Guo *et al.*, 2007). Taken together, these results show that transient exposure of nHUVEC to HG leads to persistent enhanced superoxide anion production that is further increased in response to IL-1β.

Discussion and conclusions

The present study has shown that the diabetic environment reprogrammes human fetal endothelium to respond abnormally to pro-inflammatory IL-1β through changes in the expression of genes involved in post-transcriptional mechanisms. Importantly, we identified for the first time that in endothelial cells exposed to a diabetic environment *in vivo*, miR-16 biogenesis in response to IL-1β is dysregulated concomitantly with the enhanced stabilization of COX-2 mRNA and increased production of prostanoids. $PGF_{2\alpha}$ was the most abundant prostanoid produced by dHUVEC and its concentration detected at 24 h accounted for 70% of total prostanoid levels. This prostanoid was shown to play a role in the enhanced proliferation detected in dHUVEC exposed to IL-1β as compared with nHUVEC.

Despite the fact that TP receptors are highly expressed in HUVEC (Di Francesco *et al.*, 2009), TXA_2 did not play a role in the altered proliferation detected in dHUVEC under our experimental conditions; this is possibly due to the fact that this prostanoid was produced at low concentrations (TXB_2 levels were 100-fold lower than $PGF_{2\alpha}$ levels).

In addition to endothelial cell proliferation, dysregulated biosynthesis of prostanoids in response to inflammatory mediators may play a role in the alterations of other fetoplacental endothelial cell functions reported in GDM, including impaired barrier integrity and permeability and increased angiogenesis (Leach *et al.*, 2009). Clarification of the role of different prostanoids and their specific receptors in these dysfunctional responses of fetal endothelial cells exposed to GDM went beyond the objectives of the present investigation and it deserves a targeted study.

We have shown that the exposure to GDM affects the mRNA degradation machinery of fetal endothelial cells. Interestingly, we found that IL-1β-dependent induction of miR-16 was lost in dHUVEC along with enhanced COX-2 expression. The involvement of this defective mechanism in the aberrant COX-2 expression detected in dHUVEC was demonstrated by the finding that the introduction of miR-16 into HUVEC repressed COX-2 expression. Although this study did not elucidate the precise mechanism by which GDM leads to dysregulated miR-16 biogenesis in endothelial cells, we hypothesized that an enhanced c-Myc expression may have a role in this effect. This is based on observations showing that c-Myc induces a widespread repression of miRNA expression in cancer (Chang *et al.*, 2008). In mantle cell lymphoma, c-Myc causes transcriptional repression of miR-15a/16-1 cluster gene through an interaction with the histone deacetylase HDAC3 (Zhang *et al.*, 2012).

The aberrant COX-2 expression, associated with the suppression of miR-16 and an increase in c-Myc, detected in IL-1β-stimulated dHUVEC, was induced in nHUVEC by exposing them to transient HG before their incubation with the cytokine in the presence of physiological glucose levels. Taken together these data strongly support the causal role of transient hyperglycaemia in dysregulated COX-2 expression as a result of long-lasting epigenetic changes, such as repression of miR-16 biogenesis.

The epigenetic changes caused by hyperglycaemia are probably initiated by an enhanced production of reactive oxygen species (El-Osta *et al.*, 2008). Here we found that transient exposure of nHUVEC to HG led to persistent enhanced superoxide anion production that was further increased by IL-1β. It seems unlikely that COX-2 activity played a role in superoxide anion production in HUVEC incubated without or with IL-1β. In nHUVEC transiently exposed to HG or mannitol (as osmotic control) and then maintained in normal glucose condition, the levels of COX-2 mRNA were very low (not shown). In contrast, superoxide anion generation was markedly increased by pre-incubation in HG solution compared to mannitol (Figure 6B). IL-1β is a strong inducer of COX-2 protein which, however, is detectable only after 4–6 h of incubation with the cytokine (Camacho *et al.*, 1998; Caughey *et al.*, 2001; Dixon *et al.*, 2006). In our experimental conditions, superoxide anion production was assessed after 30 min of incubation with the cytokine, when catalytically-active COX-2 is probably not present.

Our results describe a possible mechanism operating in GDM that links enhanced superoxide anion production and epigenetic changes, associated with hyperglycaemic memory, to endothelial dysfunction through dysregulated post-transcriptional control of COX-2 gene expression in response to inflammatory stimuli (Figure 7). This mechanism may partly explain the clinical data showing that early exposure to a moderately high level of hyperglycaemia has prolonged effects on diabetic complications during subsequent periods of improved glycaemia (Nathan *et al.*, 2003; 2005). Thus, in GDM, the association of conventional therapy for glycaemic control (including medications and meal planning) with agents affecting inflammatory responses and oxidative stress might lead to a more effective prevention of perinatal morbidity but also improve long-term outcomes for the mothers and their children (Figure 7).

The administration of non-steroidal anti-inflammatory drugs selective for COX-2 (coxibs) (Patrignani and Patrono, 2015) might be effective in inhibiting COX-2-dependent prostanoids induced by inflammatory stimuli. However, the concurrent inhibitory effect on constitutive biosynthesis of COX-2-dependent PGI_2 in endothelial cells by these drugs has been associated with adverse cardiovascular effects (Grosser *et al.*, 2006; Bhala *et al.*, 2013). Another limitation of conventional treatments with anti-inflammatory drugs or

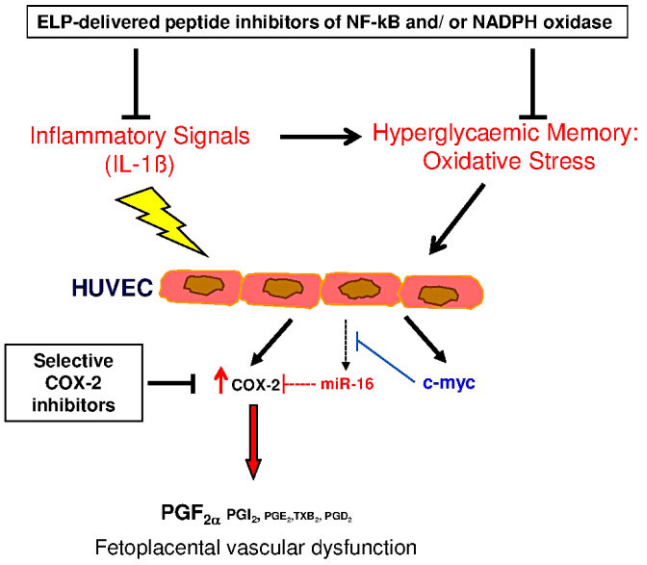

Figure 7

Mechanism involved in fetal endothelial dysfunction in GDM and possible therapeutic strategies for preventing this condition. HUVECs exposed to transient high glucose are characterized by enhanced oxidative stress that may persist even when hyperglycaemia is corrected (hyperglycaemic memory phenomenon). In the presence of circulating inflammatory mediators, endothelial oxidative stress is further increased. In this scenario, dysregulated biogenesis of miR-16 occurs and it contributes to aberrant expression of COX-2 associated with enhanced generation of prostanoids (the most abundant is the promitogenic $PGF_{2\alpha}$). The induction of c-Myc may participate in the repression of miR-16 expression. Aberrant COX-2 expression is associated with higher cellular proliferation in response to IL-1β that is abolished by a COX-2 inhibitor or FP antagonist, suggesting the involvement of COX-dependent $PGF_{2\alpha}$. The use of anti-inflammatory agents and antioxidants in association with conventional therapies used to control hyperglycaemia might help to prevent the clinical consequences of GDM. A promising strategy, under clinical investigation, is to use drug delivery vectors [such as elastin-like polypeptide (ELP)] (fused to inhibitory peptides of NF-κB (such as p50 peptide) or NADPH oxidase [such as Nox2 docking sequence (Nox2d)] that target each of these pathways in the mother while preventing fetal exposure (Bidwell and George, 2014; George *et al.*, 2014).

antioxidants is related to concerns regarding the health of the fetus. A promising strategy, currently under preclinical investigation, is the use of drug delivery vectors (such as elastin-like polypeptide) fused to inhibitory peptides of NF-κB (such as p50 peptide) or NADPH oxidase (such as Nox2 docking sequence) that target each of these pathways in the mother while preventing fetal exposure (Bidwell and George, 2014; George *et al.*, 2014). The efficacy of these novel therapeutics should be tested in appropriate animal models of GDM and in patients when they are available for human studies.

Acknowledgements

We wish to thank Mr Federico Cusinato (University of Padua, Italy) for technical assistance. This work was supported by Ministero dell'Istruzione, dell'Università e della Ricerca (MIUR) (grant PRIN 2010–2011, protocol number 2010FHH32M), Associazione Italiana per la Ricerca sul cancro (grant IG-12111 to P. P.) and National Institutes of Health (R01CA134609) (to D. A. D.). M. D., E. M. and L. D. F. received a fellowship from Abruzzo Region (Italy) for high-quality training in research (P.O. F.S.E. 2007–2013).

Author contributions

L. D. F, M. D., A. T., A. M., E. M., S. A., P. O., C. M. and G. O. performed the research. P. P., D. A. D., L. T., O. B. and G. B. N. designed the research study. S. T., A. B. and S. G. contributed to essential reagents and tools. P. P., D. A. D., L. T. and O. B. analysed the data. P. P., D. A. D., L. T. and O. B. wrote the paper. L. D. F., M. D., A. T., E. M., A. M., P. O., C. M., S. T., A. B., S. A., S. G., G. B. N., G. O., O. B., L. T., D. A. D. and P. P. revised the manuscript. L. D. F., M. D., A. T. and E. M. contributed equally.

Conflict of interest

The authors declare no conflict of interest associated with this manuscript.

References

Alexander SPH, Benson HE, Faccenda E, Pawson AJ, Sharman JL, Spedding M *et al.* (2013a). The concise guide to pharmacology 2013/14: G protein-coupled receptors. Br J Pharmacol 170: 1459–1581.

Alexander SPH, Benson HE, Faccenda E, Pawson AJ, Sharman JL, Spedding M *et al.* (2013b). The concise guide to pharmacology 2013/14: enzymes. Br J Pharmacol 170: 1797–1867.

Bhala N, Emberson J, Merhi A, Abramson S, Arber N, Baron JA *et al.* (2013). Vascular and upper gastrointestinal effects of non-steroidal anti-inflammatory drugs: meta-analyses of individual participant data from randomised trials. Lancet 382: 769–779.

Bidwell GL 3rd, George EM (2014). Maternally sequestered therapeutic polypeptides – a new approach for the management of preeclampsia. Front Pharmacol 5: 201.

Brennan CM, Steitz JA (2001). HuR and mRNA stability. Cell Mol Life Sci 58: 266–277.

Camacho M, Lopez-Belmonte J, Vila L (1998). Rate of vasoconstrictor prostanoids released by endothelial cells depends on cyclooxygenase-2 expression and prostaglandin I synthase activity. Circ Res 83: 353–365.

Caughey GE, Cleland LG, Gamble JR, James MJ (2001). Up-regulation of endothelial cyclooxygenase-2 and prostanoid synthesis by platelets. Role of thromboxane A2. J Biol Chem 276: 37839–37845.

Chang TC, Yu D, Lee YS, Wentzel EA, Arking DE, West KM *et al.* (2008). Widespread microRNA repression by Myc contributes to tumorigenesis. Nat Genet 40: 43–50.

Ciabattoni G, Pugliese F, Spaldi M, Cinotti GA, Patrono C (1979). Radioimmunoassay measurement of prostaglandins E2 and F2alpha in human urine. J Endocrinol Invest 2: 173–182.

Cooper ME, El-Osta A (2010). Epigenetics: mechanisms and implications for diabetic complications. Circ Res 107: 1403–1413.

Di Francesco L, Totani L, Dovizio M, Piccoli A, Di Francesco A, Salvatore T *et al*. (2009). Induction of prostacyclin by steady laminar shear stress suppresses tumor necrosis factor-α biosynthesis via heme oxygenase-1 in human endothelial cells. Circ Res 104: 506–513.

Dixon DA, Tolley ND, Bemis-Standoli K, Martinez ML, Weyrich AS, Morrow JD *et al*. (2006). Expression of COX-2 in platelet-monocyte interactions occurs via combinatorial regulation involving adhesion and cytokine signaling. J Clin Invest 116: 2727–2738.

Dovizio M, Maier TJ, Alberti S, Di Francesco L, Marcantoni E, Münch G *et al*. (2013). Pharmacological inhibition of platelet-tumor cell cross-talk prevents platelet-induced overexpression of cyclooxygenase-2 in HT29 human colon carcinoma cells. Mol Pharmacol 84: 25–40.

El-Osta A, Brasacchio D, Yao D, Pocai A, Jones PL, Roeder RG *et al*. (2008). Transient high glucose causes persistent epigenetic changes and altered gene expression during subsequent normoglycemia. J Exp Med 205: 2409–2417.

Figueroa R, Omar HA, Tejani N, Wolin MS (1993). Gestational diabetes alters human placental vascular responses to changes in oxygen tension. Am J Obstet Gynecol 168: 1616–1622.

George EM, Liu H, Robinson GG, Bidwell GL (2014). A polypeptide drug carrier for maternal delivery and prevention of fetal exposure. J Drug Target 22: 935–947.

Griffin BW, Klimko P, Crider JY, Sharif NA (1999). AL-8810: a novel prostaglandin F2 alpha analog with selective antagonist effects at the prostaglandin F2 alpha (FP) receptor. J Pharmacol Exp Ther 290: 1278–1284.

Grosser T, Fries S, FitzGerald GA (2006). Biological basis for the cardiovascular consequences of COX-2 inhibition: therapeutic challenges and opportunities. J Clin Invest 116: 4–15.

Guo Z, Xia Z, Jiang J, McNeill JH (2007). Downregulation of NADPH oxidase, antioxidant enzymes, and inflammatory markers in the heart of streptozotocin-induced diabetic rats by N-acetyl-L-cysteine. Am J Physiol Heart Circ Physiol 292: H1728–H1736.

Hay WW Jr (2006). Placental-fetal glucose exchange and fetal glucose metabolism. Trans Am Clin Climatol Assoc 117: 321–340.

International Association of Diabetes and Pregnancy Study Groups Consensus Panel (2010). International association of diabetes and pregnancy study groups recommendations on the diagnosis and classification of hyperglycemia in pregnancy. Diabetes Care 33: 676–682.

Jaffe EA, Nachman RL, Becker CG, Minick CR (1973). Culture of human endothelial cells derived from umbilical veins: identification by morphologic and immunologic criteria. J Clin Invest 52: 2745–2756.

Jayaraman S (2012). Epigenetic mechanisms of metabolic memory in diabetes. Circ Res 110: 1039–1041.

Leach L (2011). Placental vascular dysfunction in diabetic pregnancies: intimations of fetal cardiovascular disease? Microcirculation 18: 263–269.

Leach L, Taylor A, Sciota F (2009). Vascular dysfunction in the diabetic placenta: causes and consequences. J Anat 215: 69–76.

Marco LJ, McCloskey K, Vuillermin PJ, Burgner D, Said J, Ponsonby AL (2012). Cardiovascular disease risk in the offspring of diabetic women: the impact of the intrauterine environment. Exp Diabetes Res 2012: 565160.

Moore AE, Young LE, Dixon DA (2011). MicroRNA and AU-rich element regulation of prostaglandin synthesis. Cancer Metastasis Rev 30: 419–435.

Mosmann T (1983). Rapid colorimetric assay for cellular growth and survival: application to proliferation and cytotoxicity assays. J Immunol Methods 65: 55–63.

Nathan DM, Lachin J, Cleary P, Orchard T, Brillon DJ, Backlund JY *et al*. (2003). Intensive diabetes therapy and carotid intima-media thickness in type 1 diabetes mellitus. N Engl J Med 348: 2294–2303.

Nathan DM, Cleary PA, Backlund JY, Genuth SM, Lachin JM, Orchard TJ *et al*. (2005). Intensive diabetes treatment and cardiovascular disease in patients with type 1 diabetes. N Engl J Med 353: 2643–2653.

Ogletree ML, Harris DN, Greenberg R, Haslanger MF, Nakane M (1985). Pharmacological actions of SQ 29 548, a novel selective thromboxane antagonist. J Pharmacol Exp Ther 234: 435–441.

Panara MR, Greco A, Santini G, Sciulli MG, Rotondo MT, Padovano R *et al*. (1995). Effects of the novel anti-inflammatory compounds, N-[2-(cyclohexyloxy)-4-nitrophenyl] methanesulphonamide (NS-398) and 5-methanesulphonamido-6-(2,4-difluorothio-phenyl)-1-inda none (L-745 337), on the cyclo-oxygenase activity of human blood prostaglandin endoperoxide synthases. Br J Pharmacol 116: 2429–2434.

Patrignani P, Patrono C (2015). Cyclooxygenase inhibitors: from pharmacology to clinical read-outs. Biochim Biophys Acta 1851: 422–432.

Patrignani P, Filabozzi P, Catella F, Pugliese F, Patrono C (1984). Differential effects of dazoxiben, a selective thromboxane-synthase inhibitor, on platelet and renal prostaglandin-endoperoxide metabolism. J Pharmacol Exp Ther 228: 472–477.

Patrignani P, Panara MR, Greco A, Fusco O, Natoli C, Iacobelli S *et al*. (1994). Biochemical and pharmacological characterization of the cyclooxygenase activity of human blood prostaglandin endoperoxide synthases. J Pharmacol Exp Ther 271: 1705–1712.

Patrono C, Pugliese F, Ciabattoni G, Patrignani P, Maseri A, Chierchia S *et al*. (1982). Evidence for a direct stimulatory effect of prostacyclin on renin release in man. J Clin Invest 69: 231–239.

Pawson AJ, Sharman JL, Benson HE, Faccenda E, Alexander SP, Buneman OP *et al*.; NC-IUPHAR (2014). The IUPHAR/BPS Guide to PHARMACOLOGY: an expert-driven knowledgebase of drug targets and their ligands. Nucl. Acids Res 42 (Database Issue): D1098–D1106.

Radaelli T, Varastehpour A, Catalano P, Hauguel-de Mouzon S (2003). Gestational diabetes induces placental genes for chronic stress and inflammatory pathways. Diabetes 52: 2951–2958.

Sexl V, Mancusi G, Baumgartner-Parzer S, Schütz W, Freissmuth M (1995). Stimulation of human umbilical vein endothelial cell proliferation by A2-adenosine and beta 2-adrenoceptors. Br J Pharmacol 114: n1577–n1586.

Sobrevia L, Abarzúa F, Nien JK, Salomón C, Westermeier F, Puebla C *et al*. (2011). Review: differential placental macrovascular and microvascular endothelial dysfunction in gestational diabetes. Placenta 32: S159–S164.

Sun X, Icli B, Wara AK, Belkin N, He S, Kobzik L *et al*. (2012). MicroRNA-181b regulates NF-κB-mediated vascular inflammation. J Clin Invest 122: 1973–1990.

Trenti A, Grumati P, Cusinato F, Orso G, Bonaldo P, Trevisi L (2014). Cardiac glycoside ouabain induces autophagic cell death in non-small cell lung cancer cells via a JNK-dependent decrease of Bcl-2. Biochem Pharmacol 89: 197–209.

Trevisi L, Pighin I, Bazzan S, Luciani S (2006). Inhibition of 3-(4.5-dimethylthiazol-2-yl)-2.5-diphenyltetrazolium bromide (MTT) endocytosis by ouabain in human endothelial cells. FEBS Lett 580: 2769–2773.

Trevisi L, Bertoldo A, Agnoletto L, Poggiani C, Cusinato F, Luciani S (2010). Antiapoptotic and proliferative effects of low concentrations of 7β-hydroxycholesterol in human endothelial cells via ERK activation. J Vasc Res 47: 241–251.

Vitoratos N, Valsamakis G, Mastorakos G, Boutsiadis A, Salakos N, Kouskouni E *et al*. (2008). Pre- and early post-partum adiponectin and interleukin-1beta levels in women with and without gestational diabetes. Hormones (Athens) 7: 230–236.

Williams MR, Kataoka N, Sakurai Y, Powers CM, Eskin SG, McIntire LV (2008). Gene expression of endothelial cells due to interleukin-1 beta stimulation and neutrophil transmigration. Endothelium 15: 73–165.

Yessoufou A, Moutairou K (2011). Maternal diabetes in pregnancy: early and long-term outcomes on the offspring and the concept of 'metabolic memory'. Exp Diabetes Res 2011: 218598.

Young LE, Moore AE, Sokol L, Meisner-Kober N, Dixon DA (2012). The mRNA stability factor HuR inhibits microRNA-16 targeting of COX-2. Mol Cancer Res 10: 167–180.

Zhang E, Wu Y (2014). Metabolic memory: mechanisms and implications for diabetic vasculopathies. Sci China Life Sci 57: 845–851.

Zhang X, Chen X, Lin J, Lwin T, Wright G, Moscinski LC *et al*. (2012). Myc represses miR-15a/miR-16-1 expression through recruitment of HDAC3 in mantle cell and other non-Hodgkin B-cell lymphomas. Oncogene 31: 3002–3008.

Supporting information

Additional Supporting Information may be found in the online version of this article at the publisher's web-site:

http://dx.doi.org/10.1111/bph.13241

Figure S1 COX-1 protein expression in nHUVEC and dHUVEC at baseline and in response to IL-1β. COX-1 levels in HUVEC under basal condition or stimulated with IL-1β (5 ng·mL^{-1}) for 6 and 24 h were assessed by Western blot. β-Actin was used as loading control.

Figure S2 HuR localization in nHUVEC and dHUVEC at baseline and in response to IL-1β. HuR localization was assessed by confocal microscopy analysis in nHUVEC or dHUVEC cultured in the absence or in the presence of IL-1β (5 ng·mL^{-1}) for 24 h. Immunostaining of HuR is shown in green and propidium iodide (PI, nuclear marker) in red. Scale bar, 10 μm.